SPE 94140

Quantification of Uncertainty in Relative Permeability for Coarse-Scale Reservoir Simulation

H. Okano, SPE, Heriot-Watt U. and Japan Oil, Gas, and Metals Natl. Corp.; G.E. Pickup, SPE, and M.A. Christie, SPE, Heriot-Watt U.; S. Subbey, SPE, Inst. of Marine Research; M. Sambridge, Australian Natl. U.; and H. Monfared, SPE, Heriot-Watt U. and Natl. Iranian Oil Co.

This paper was prepared for presentation at the SPE Europec/EAGE Annual Conference held in Madrid, Spain, 13-16 June 2005.

Abstract

Reservoir simulation to predict production performance requires two steps: one is history-matching, and the other is uncertainty quantification in forecasting. In the process of history-matching, rock relative permeability curves are often altered to reproduce production data. However, guidelines for changing the shape of the curves have not been clearly established. The aim of this paper is to clarify the possible influence of relative permeabilities on reservoir simulation using the uncertainty envelope.

We propose a method for adjusting the shape of relative permeability curves during history-matching at the coarse scale, using the Neighbourhood Approximation algorithm and B-spline parameterisation. After generating multiple history-matched models, we quantify the uncertainty envelope in a Bayesian framework. Our approach aims at encapsulating sub-grid heterogeneity in multi-phase functions directly in the coarse-scale model, and predicting uncertainty. In this sense, the framework differs from conventional procedures which perturb fine-scale features, upscale the models and evaluate each performance. In addition, B-spline parameterisation is flexible allowing the capture of local features in the relative permeability curves. The results of synthetic cases showed that the lack of knowledge of the subgrid permeability and the insufficient production data provoked a substantial amount of uncertainty in reservoir performance forecasting.

Introduction

Reservoir simulation is routinely employed in the prediction of reservoir performance under different depletion and operating scenarios. This practical use of reservoir simulation requires two steps: one is history-matching, and the other is uncertainty quantification in forecasting. In the traditional approach, a single history-matched model, conditioned to production data, is obtained, and is used to forecast future production profiles. Since the history-matching is non-unique, the forecast production profiles are uncertain. Recently, in order to take account of the non-uniqueness of the inverse problem, a new methodology for uncertainty quantification has been introduced to the petroleum industry. The Markov Chain Monte Carlo method has been adopted by [1, 2, 3, 4], along with the Neighbourhood Approximation [5, 6], in order to investigate parameter space.

Here, the requirement for reservoir modelling is to generate multiple history-matched models which encapsulate the effect of the detailed features in a reservoir. In general, as the cell size of a model gets smaller, the accuracy for capturing the details improves. In reservoir modelling studies, the geostatistical approach has been employed to generate multiple realisations at the fine scale. Then, because simulation of the fine-scale model is usually too time consuming, the number of cells is reduced by upscaling to conduct history-matching. However, upscaling techniques have some problematic aspects in real situations. For example, given complete details of the fine-scale features, two-phase upscaling could be performed to calculate pseudo relative permeabilities for every coarse-grid cell in each direction. The pseudos then require grouping into a limited number of tabular functions for coarse-scale simulation, [7, 8]. Unfortunately, this procedure is not feasible, as it is time consuming and results may not be robust. On top of those issues on upscaling, the task of evaluating multiple realisations of geostatistical models still remains a research issue. For example, if you try to adjust a correlation length in geostatistical simulations to history-match the model, you need to take into account the variance of the multiple realisations as well.

The approach proposed in this paper aims at encapsulating sub-grid heterogeneity in multi-phase functions directly at the coarse-scale, and predicting uncertainty. The proposed framework also aims at avoiding those problems in the conventional approaches discussed above which perturb fine-scale features, upscale the models and evaluate each performance.

Furthermore, during the process of history-matching, rock relative permeability curves are often altered to reproduce production data, although guidelines for changing the shape of the curves have not been clearly established. In this paper, we employ B-spline functions to parameterise relative permeabilities and try to clarify their influence on the uncertainty estimation. B-spline parameterisation is flexible allowing the capture of local features in the relative permeability curves, [9, 10, 11, 12].

We use a synthetic fine-scale model, which is small enough to conduct flow simulations, and we assume that this is the "truth". After generating multiple history-matched models, we quantify the uncertainty envelope in a Bayesian framework. We compare the pseudofunctions as the representative of the truth with the relative permeabilities estimated using the history-matching procedure, at the coarse-scale. This comparison allows us to examine how reasonable the estimation of relative permeabilities is, in terms of encapsulating small-scale heterogeneity.

Theory for History-Matching and Uncertainty Quantification

Bayesian Inference. Bayesian inference, [13], can be described by the following equation in the context of history-matching.

$$\text{prob}(\mathbf{m}|\mathbf{o}) = \frac{\text{prob}(\mathbf{o}|\mathbf{m}) \times \text{prob}(\mathbf{m})}{\int \text{prob}(\mathbf{o}|\mathbf{m}) \times \text{prob}(\mathbf{m})\, d\mathbf{m}}, \tag{1}$$

where $\int d\mathbf{m} = \int\int \ldots \int dm_1 dm_2 \ldots dm_{N_m}$ for $\mathbf{m} = (m_1, m_2, \ldots, m_{N_m})$. The vector $\mathbf{m}$ represents a set of parameters which describes a reservoir model and the vector $\mathbf{o}$ represents a set of observed data in the reservoir. Here, the probability of the vector means the joint probability for all components in the vector. The term prob($\mathbf{m}$) in Equation (1) is the prior probability which represents our state of knowledge about the model before making an observation, and the posterior probability prob($\mathbf{m}|\mathbf{o}$) represents our state of knowledge about model after making an observation. The likelihood function, prob($\mathbf{o}|\mathbf{m}$), is the probability that an observation is correct given the model. This function is used to update the prior probability. It implies how we should change the state of knowledge of prob($\mathbf{m}$) as a result of making an observation prob($\mathbf{o}|\mathbf{m}$). The denominator in the right-hand side is referred as the normalisation constant, since the sum of the posterior probability over all possible models must equal one. Equation (1) has been adopted for uncertainty quantification in reservoir simulation, [1, 2, 3, 4]. In order to conduct Bayesian inference, we may need to integrate over a high-dimensional probability distribution. Markov Chain Monte Carlo (MCMC), which is Monte Carlo integration using Markov chains, is widely used to overcome the numerical difficulties in many applications, [14].

Neighbourhood Approximation (NA) Algorithm and NA-Bayes Algorithm. The Neighbourhood Approximation (NA) algorithm is a stochastic sampling algorithm, which was originally developed to solve an inverse problem in seismology, [5], and the application of the NA-algorithm to history-matching has recently been introduced to the petroleum industry, [15, 1, 2, 3, 4]. The algorithm uses information obtained from previous runs to bias the sampling of model parameters to regions of parameter space where a good fit is likely. In this way it attempts to overcome a main concern of stochastic sampling, namely poor convergence.

The algorithm explores parameter space using Voronoi cells. Multiple history-matched models are generated in parameter space according to the following rule. At each iterative stage, the algorithm generates n_s models and calculates their misfit values. Then all the models, including those previously generated, are ranked to determine the best n_r cells. n_s new models are then generated in these n_r cells, i.e., by placing n_s/n_r models in each cell. The philosophy behind the algorithm is that the misfit of each of the previous models is representative of the region of its neighbourhood, defined by its Voronoi cell. Therefore at each iteration step, new samples are concentrated in the neighbourhoods surrounding the better data-fitting models. Thus the objective of the algorithm is to bias the sampling to good history-matching regions of the parameter space. By its nature, the algorithm exploits information in all previous models to selectively sample parameter space. The two parameters that control the algorithm are n_s and n_r. Indeed, these are the only tuning parameters that control the performance of the algorithm. The amount of exploration and exploitation performed by the algorithm is dependent on these parameters.

Sambridge [6] also applied this Neighbourhood Approximation to the sampling from the posterior probability distribution (PPD) in Bayesian framework, (NA-Bayes Algorithm). Suppose that we have obtained the information on the PPD during the history-matching with NA. Then, we use MCMC to evaluate the posterior expectation without conducting any additional flow simulations. By simply setting the known PPD of each model to be constant inside its Voronoi cell, we can construct an approximate PPD from a fixed ensemble. This approximation allows us to avoid calculating the real PPD of the new proposed models at each step of MCMC. Further details of the NA-Bayes Algorithm are described in Appendix B. In this paper we used this scheme of the MCMC with the Neighbourhood Approximation to evaluate the posterior expectation and P10 and P90 cut-offs, [1, 2, 3, 4].

Model and Problem Description

Fine-Scale Model, Coarse-Scale Model and Observed Data. We assume a water flooding scenario in an oil reservoir. We generated a 2D truth model, which is shown in Figures 1 (permeability distribution) and 2 (histogram). This is also referred to as the fine-scale model, in contrast to the coarse-scale model used for history matching (Figure 3). There are 55×275×1 cells in this fine-scale model, each of size 5m×5m×20m. Porosity is 0.2 and is uniform throughout the model. The permeability was generated by Sequential Gaussian Simulation (SGS), [16], and was conditioned to data for 2 vertical wells (200mD). The correlation length is 135 m in the Y-direction (North) and 67.5 m in the X-direction (East). The Gaussian random numbers were transformed to logarithmic permeabilities, ln(k), by multiplying them by the standard deviation and adding the mean. In this case, the mean and standard deviation of ln(k) were assumed to be 5.3 and 0.5 respectively. Relative permeability for the truth model was assigned by adopting Corey-type rock curves [17] with an exponent of 2, i.e.,

$$K_{ro}(S_w) = ([S_w - S_{wc}]/[1 - S_{wc} - S_{or}])^2 , \quad (2)$$
$$K_{rw}(S_w) = ([1 - S_w - S_{or}]/[1 - S_{wc} - S_{or}])^2 , \quad (3)$$
$$S_{wc} = S_{or} = 0.2, \quad (4)$$

where $K_{ro}(S_w)$ and $K_{rw}(S_w)$ denote oil and water relative permeabilities, S_w is water saturation, S_{wc} is connate water saturation and S_{or} is residual oil saturation. Oil viscosity is approximately 1.0 [cp] and water viscosity is 0.3 [cp]. The other parameters for the fluid properties are the same as those in the second data set of the 10th SPE Comparative Solution Project [18].

The coarse-scale model (Figure 3) was employed for multiple flow simulations for history-matching. The coarse cell size is 275m×275m×20m and the number of cells is 1×5×1. The producer and water injector wells were placed at the centres of the edge coarse cells, and the well positions in the coarse-scale model are exactly the same as those in the fine-scale (truth) model. The boundary conditions were the same in both scale models: the producer well was controlled by a bottom hole pressure (BHP) of 400 [bar], the injector well was controlled by a rate of 330.0 [m^3/day] (reservoir conditions) and BHP limit of 689.48 [bar], and the sides of the model were sealed.

The main task of this paper is to estimate relative permeabilities at the coarse scale through history-matching rather than varying parameters at the fine scale. The correlation length of the truth model is less than half of a coarse-scale cell (275m). In other words, each coarse-scale cell contains subgrid heterogeneity for which the range is smaller than a cell. In most models, a range of coarse-scale relative permeability curves is required to take account of fine-scale effects. Also, the relative permeability usually depends on distance from the wells in coarse-scale models, [19]. In this study, however, we have chosen to concentrate on the second and third cells from the injector cell as our target cells for history matching, and we refer to them below as Cell 2 and Cell 3, respectively (Figure 3). For simplification, although the truth model is unknown in real situations, we used the truth model to fix all parameters other than relative permeabilities of Cells 2 and 3. Details of the coarse-scale model are provided in Appendix B.

We history-match the model by adjusting a single set of relative permeability curves for those two cells. For comparison, we also calculated two sets of pseudofunctions for the two cells using the PVW method (ECLIPSE PSEUDO package [20]). Figures 4 and 5 show the production performance of the fine-scale model, the coarse-scale model with rock curves and the coarse-scale model with pseudofunctions. The oil rate and injector bottom hole pressure (BHP) of the coarse-scale model with pseudofunctions coincide with those of the fine-scale model, whereas the coarse-scale model with rock curve fails to reproduce the fine-scale profiles in some intervals. In the section below, we replace the two sets of pseudofunctions with the one set of optimised relative permeability curves and compare the results.

We use the oil rate and injector BHP as history data. To create a more realistic case, we added uncorrelated random noise to the fine-scale data in the following way. We drew a set of random numbers rnd from a normal distribution, $rnd \sim N(0, 1)$, and defined Observed Oil Rate and Observed Injector BHP:

$$\text{(Observed Oil Rate)} = \text{(Fine model Oil Rate)} + \sigma_q \, rnd, \quad (5)$$
$$\text{(Observed Inj. BHP)} = \text{(Fine model Inj. BHP)} + \sigma_p \, rnd, \quad (6)$$

where σ_q and σ_p are the standard deviations of the data errors for the oil rate and injector BHP respectively. In this paper, we assume that $\sigma_q = 15.0\,[m^3/\text{day}]$ and $\sigma_p = 1.0\,[\text{bar}]$. We denote the fine-scale data as the truth in the sections below. Then we use data for 1350 days as history data. The task is to history-match the coarse-scale model to the observed data, by adjusting the relative permeability curves. Finally, we forecast the production performance to 4000 days, and quantify the uncertainty in our forecast.

Misfit Definition. In this paper we assume that the data errors are independently and identically distributed (IID). A more advanced definition of error models is discussed in [21]. We define the likelihood function in the following Gaussian expression.

$$\text{prob}(\mathbf{o}|\mathbf{m}) \quad \propto \quad \prod_{k=1}^{N} \exp\left(-\frac{(q_k - q'_k)^2}{2\sigma_q^2} - \frac{(p_k - p'_k)^2}{2\sigma_p^2}\right). \quad (7)$$

Here q' and p' represent the simulated oil rate and BHP respectively, and q and p represent the observed oil rate and BHP respectively. The subscript $k = 1, 2, \ldots, N$ represents the time step. N is the total number of the time series data. As above, σ_q and σ_p are the standard deviations of the data errors. Accordingly, the measure of misfit, M, as an object function can be given in the least square sense by the following equation.

$$M = \sum_{k=1}^{N} \left(\frac{(q_k - q'_k)^2}{2\sigma_q^2} + \frac{(p_k - p'_k)^2}{2\sigma_p^2}\right). \quad (8)$$

Parameterisation for Relative Permeabilities

Issues on Relative Permeabilities. Relative permeability is defined as the ratio of phase permeability to absolute permeability and is assumed to be a function of saturation, [22, 23]. Relative permeability curves for a core sample can be obtained from steady-state or unsteady-state core flooding experiments. The unsteady-state method is usually preferred to the steady-state method because of the time required. The JBN method [24] may be used to calculate relative permeabilities from unsteady-state displacements, using the saturation and fractional flows measured at the effluent end of the core. Alternatively, relative permeabilities may be derived by history-matching at the core scale, so that the simulation result from a numerical model of the core flooding matches the observed data.

It is not appropriate to use relative permeability curves obtained from core flooding experiments directly in coarse-scale simulation models. Ideally they should be upscaled to account for geological heterogeneity, fluid forces and numerical gridding effects. However, two-phase upscaling is time consuming and is not robust [25, 26]. An alternative approach is to obtain relative permeabilities directly at the coarse scale by history-matching, and this is the approach taken here.

B-spline Function for Relative Permeabilities at the Coarse Scale. B-splines are piecewise polynomials which form useful local basis elements for spline spaces, [27]. The shapes of the basis elements are determined by a knot-vector, which is a partition of the interval on which the function is to be defined. The advantage is that any continuous function can be approximated by polynomial splines with sufficient number of knots. Introduction of knots in an interval gives flexibility in defining the function over that interval. Whereas the power law (Corey) [17] and exponential function (Chierici) [28, 29] have only a small number of parameters to control the shape of the whole relative permeability curve, B-spline functions can have more parameters each of which control a limited part of the curve, [9, 10, 11, 12]. This characteristic of B-spline function leads to the local flexibility for adjusting curves during the history-matching. In this paper, we parameterise the relative permeability with the fourth order (cubic) B-spline function in the following way.

$$K_{ri}(S_w) = \sum_{j=1}^{n} c_j^i N_j^4(S_w) \quad \text{for } i = o, w, \quad (9)$$

where $K_{ri}(S_w)$ is the relative permeability for the i-th phase, $N_j^4(S_w)$ is the j-th normalised cubic B-spline basis function, c_j^i is the j-th B-spline coefficient for the i-th phase and n is the B-spline dimension, [27, 11].

It is important to select appropriate parameters for the spline function (number of dimensions and knot spacing) to produce a realistic shape for the relative permeabilities, [10, 12]. Preliminary tests for nearly linear water flooding cases were performed on 2D stochastic models, which were upscaled using dynamic upscaling (PVW method, [20]). These tests showed that when a model was upscaled, the pseudo relative permeabilities were shifted to the right compared with the rock curve to compensate for numerical dispersion, [30, 31]. On the contrary, if there is a long correlation in the principal flow direction, the pseudo relative permeabilities are shifted to the left to represent early breakthrough. According to these results, we decided to use 6 B-spline Basis functions (6-dimension), with nonuniformly spaced knots at water saturations of 0.20, 0.35, 0.50 and 0.80. This allows us to represent complex pseudos functions, especially in the saturation range between 0.2 and 0.5. The B-spline basis functions are shown in Figure 6.

Prior Distribution and NA-Algorithm Parameters. We based the prior information on both the rock curves and the scale-change effect in order to narrow down the parameter space of B-spline coefficients. This tends to reduce the computational cost for history-matching, i.e. the number of flow simulations required to converge to the best fit regions in the parameter space. We fixed the minimum and maximum values for each B-spline coefficient as shown in Table 1. The range of relative permeabilities corresponding to the minimum and maximum coefficients are shown in Figure 7.

In real situations we can not calculate pseudofunctions for thousands of fine-scale models. So here we just roughly speculated the possible parameter ranges, rather than abstracting the detailed features, of the pseudofunctions for a variety of models which have different correlation lengths. Figure 7 shows the pseudofunctions, calculated for a range of correlation lengths: $0 \leq \lambda_X \leq 67.5$ m, and $0 \leq \lambda_Y \leq 1350$ m. The total number of models generated by SGSIM is 96, 16 cases times

6 realisations for each case, including the truth model. The standard deviation and mean assumed in the transformation to logarithmic permeabilities are the same as those for the truth model explained above. Figure 7 also includes a homogeneous model in which the only effect is the compensation of numerical dispersion. Figure 7 indicates that we selected the minimum and maximum values of B-spline coefficients in advance so that we could narrow down the parameter space and cover a wide variety of pseudofunctions encapsulating the possible fine-scale features.

As shown in Table 1, we use history-matching to set the relative permeabilities by adjusting 8 parameters, 4 for each phase, within the specified ranges. In the section below, parameters 1 to 4 denote c_2^o to c_5^o for the oil phase. In the same manner, parameters 5 to 8 denote c_2^w to c_5^w for the water phase. Since NA-algorithm samples parameters within the prior ranges, it can be said that the resultant ensemble is automatically truncated by the edges of uniform prior distribution. Then, the next task is to sample the resulting ensemble using MCMC with Neighbourhood Approximation. This step of MCMC is referred to as sampling from posterior probability distribution (PPD). Here, because of the Neighbourhood Approximation, the products of likelihood and prior distribution, $\text{prob}(\mathbf{o}|\mathbf{m}) \times \text{prob}(\mathbf{m})$, of the second ensemble have already been evaluated at the first step.

The characteristic of NA-sampling, in terms of exploration and exploitation, is largely controlled by the two tuning parameters n_s and n_r, [5]. The values of n_s and n_r used in this paper were 96 and 48 respectively, because we aimed at the exploratory sampling within the limitation of computational cost.

Results of Estimating Relative Permeability and Production Performance

Quantifying uncertainty requires several hundreds to thousands of realizations. In this paper we present results where we have used the NA-algorithm to generate 7296 models by sampling a 8-dimensional parameter space. To quantify the uncertainty in our predictions, we ran a long chain of the MCMC algorithm on the misfit surface, collected 100000 models in total and performed a Bayes update of the probabilities. We monitored the frequency of visits to each Voronoi cell during the random walk. Thus we were able to calculate the relative probability of each model in the ensemble. Since the MCMC algorithm samples from the posterior distribution, through the product of the likelihood and the prior distribution, the calculated probability is representative of the posterior probability of each model. Using the probability of each model, we determined not only the expectation, but also P10 and P90 cut-offs for each of the estimated relative permeabilities and production profiles.

We used the observed data up to 1350 days, corresponding to 38.9% of water cut, for history-matching and quantified the uncertainty up to 4000 days. The results are shown in Figures 8 to 15. Figure 8 confirms the convergence of NA-sampling to regions of good fit. Figure 9 indicates that the optimised relative permeability curves are similar to the pseudofunctions. In other words, the two pseudofunctions could be grouped into one set of curves. Figures 10 and 11 illustrate the history-matching results for the oil rate and the injector BHP. In this case, the simulated oil rate and injector BHP seem to almost overlap with the truth profile. Figure 12 plots the 1-dimensional posterior probability distribution for each of the parameters. These are projections of the multidimensional posterior probability distribution onto each of the 8 parameter axes. As shown in Figure 12, the marginal distributions of some parameters, e.g. Parameter 1, Parameter 4 and Parameter 8, have wide shapes rather than the narrow skewed shapes seen in the other parameters. The wide PPD means that the parameters may not be fixed through history-matching because of the lack of adequate information or noisy observed data. Also, the features of the wide PPD caused a wide uncertainty envelope in the relative permeability curves, Figure 13, and in the production profiles during the prediction period, Figures 14 and 15. The spread in oil rate, between the P10 and P90 values, is relatively small. However, in a real reservoir, this could represent a significant difference in cumulative oil, and shows the importance of taking uncertainty into account when planning the development of a field.

Discussion

Recently a new concept of "Top-down reservoir modelling" has been discussed, [32]. The way of thinking is to start at the coarse scale, keep the model simple and add the detailed features later to evaluate the uncertainty, for instance using downscaling methods, [33, 34, 35]. In the context of "Top-down reservoir modelling", the procedure proposed in this paper can contribute to history-matching and uncertainty prediction at the coarse scale without refining it. For example, suppose that you are given a roughly history-matched model, and the large-scale heterogeneity, such as channel delineation and fault compartmentalisation, has already been fixed. The following task is to take into account the small-scale heterogeneity which the main representations of the simple model may miss. Here, it is an inevitable bar to appropriate modelling that we do not know the true fine-scale permeability distribution. In such situations, our procedure shows how it may be possible to encapsulate small-scale flow phenomenon in relative permeabilities of the coarse-scale cells, using the flexible B-spline parameterisation and the NA-sampler.

Conclusion

This paper has demonstrated a methodology for adjusting relative permeabilities to generate history-matched models at a coarse scale, and quantifying uncertainty in reservoir performance forecast using the Neighbourhood Approximation algorithm and Markov Chain Monte Carlo.

In order to conduct the numerical experiments, we used a synthetic data set for which the true solution is known. We examined the optimised relative permeabilities and their uncertainty envelope by comparing them with pseudofunctions that were generated from the truth model. The optimised relative permeabilities and their uncertainty envelope were found to resemble pseudofunctions. This evidence indicated that the estimated relative permeability curves would encapsulate the fine-scale flow phenomenon through the local features of the B-spline functions. The key is to evaluate the relative permeabilities so that they can represent both the sub-grid heterogeneity and the numerical coarse-scale effect. One of the issues which remains as future research is how to decrease the number of parameters or limit their ranges to decrease computational cost.

Basically, it is the essential and practical task of reservoir simulation to speculate on the future performance from only a limited number of production data. Therefore, you need to understand how the relative permeabilities affect the overall production performance, whatever procedure is used to adjust the curves during history-matching. From this requirement, our results clarified the possible influence of relative permeabilities on the envelope of uncertainty in production.

Acknowledgement

We should like to thank JOGMEC for sponsoring Hirofumi Okano, NIOC for sponsoring Hashem Monfared and the following companies for sponsoring the Uncertainty and Upscaling Projects: Anadarko, BG, BP, ConocoPhillips, the DTI, Eni, JOGMEC, Landmark Graphics, Petronas, Statoil, and Shell. We should also like to thank Schlumberger for the use of the ECLIPSE and PSEUDO Package.

Nomenclature

c_j^o, c_j^w = j-th B-spline coefficients for oil and water
i = index for phases of oil and water
j = index for B-spline coefficients or basis functions
k = index for time steps
$K_{ro}(S_w)$, $K_{rw}(S_w)$ = oil and water relative permeabilities
$\mathbf{m}$ = vector of model parameters
M = measure of misfit
N_m = total number of model parameters
N = total number of time series data for each p and q
n = B-spline dimension
$N_j^4(S_w)$ = j-th normalised cubic B-spline basis function
$N(mean, standard\ deviation)$ = normal distribution
n_r = number of refinements at each iteration in NA-algorithm
n_s = number of samples at each iteration in NA-algorithm
$\mathbf{o}$ = vector of observed data
prob($\mathbf{m}$) = prior probability of model parameters
prob($\mathbf{m}|\mathbf{o}$) = posterior probability of model parameters
prob($\mathbf{o}|\mathbf{m}$) = likelihood function of model parameters
p = injector bottom hole pressure, $\mathrm{mL^{-1}t^{-2}}$, bar
p'_k, q'_k = simulated data at time "k" for p and q
p_k, q_k = observed data at time "k" for p and q
q = oil rate, $\mathrm{L^3t^{-1}}$, $\mathrm{m^3/day}$
rnd = random numbers
S_w = water saturation
S_{or} = residual oil saturation
S_{wc} = connate water saturation
σ_p, σ_q = standard deviations of data errors for p and q
λ_X, λ_Y = correlation length in X-direction and Y-direction

References

1. Christie, M., Subbey, S. and Sambridge, M.: “Prediction under Uncertainty in Reservoir Modeling,” presented at the 2002 European Conference on the Mathematics of Oil Recovery, Freiberg, September 3-6.
2. Christie, M., Subbey, S., Sambridge, M. and Thiele, M.: “Quantifying Prediction Uncertainty in Reservoir Modelling using Streamline Simulation,” presented at the 2002 ASCE Engineering Mechanics Conference, June.
3. Subbey, S., Christie, M. and Sambridge, M.: “A Strategy for Rapid Quantification of Uncertainty in Reservoir Performance Prediction,” paper SPE 79678 presented at the 2003 SPE Reservoir Simulation Symposium, Houston, February.
4. Subbey, S., Christie, M. and Sambridge, M.: “Uncertainty Reduction in Reservoir Modelling,” *Fluid Flow and Transport in Porous Media: Mathematical and Numerical Treatment*, eds. Z. Chen and R. Ewing, American Mathematical Society Contemporary Mathematics Monograph (2002) .
5. Sambridge, M.: “Geophysical Inversion with a Neighbourhood Algorithm -I.: Searching a Parameter Space,” *Geophysical Journal International* (1999) **138**, 479.
6. Sambridge, M.: “Geophysical Inversion with a Neighbourhood Algorithm -II.: Appraising the Ensemble,” *Geophysical Journal International* (1999) **138**, 727.
7. Christie, M.A.: “Upscaling for Reservoir Simulation,” *JPT* (November 1996) **48**, 1004.
8. Dupouy, P., Barker, J.W. and Valois, J.: “Grouping Pseudo Relative Permeability Curves,” *IN SITU* (1998) **22**, 1.
9. Kulkarni, K.N. and Datta-Gupta, A.: “Estimating Relative Permeability from Pruduction Data: A Streamline Approach,” paper SPE 56751 presented at the 1999 SPE Annual Technical Conference and Exhibition, Houston, October 3-6.
10. Richmond, P.C. and Watson, A.T.: “Estimation of Multiphase Flow Functions From Displacement Experiments,” *SPERE* (February 1990) , 121.

11. Subbey, S., Monfared, H., Christie, M. and Sambridge, M.: "Quantifying Uncertainty in Flow Functions Derived from SCAL Data: USS Relative Permeability and Capillary Pressure," *Transport in Porous Media* (2005) accepted for publication.

12. Watson, A.T., Richmond, P.C., Kerig, P.D. and Tao, T.M.: "A Regression-Based Method for Estimating Relative Permeabilities From Displacement Experiments," *SPERE* (August 1988) **3**, 953.

13. Sivia, D.S.: *Data Analysis: A Bayesian Tutorial*, Oxford University Press, Inc., New York (1996).

14. Gilks, W.R., Richardson, S. and Spiegelhalter, D.J.: *Markov Chain Monte Carlo in Practice*, Chapman & Hall, London (1996).

15. Christie, M., MacBeth, C. and Subbey, S.: "Multiple History-matched Models for Teal South," *The Leading Edge* (March 2002) **21**, 286.

16. Deutsch, C.V. and Journel, A.G.: *GSLIB: Geostatistical Software Library and User's Guide*, Oxford University Press, Inc, New York, second edition (1998).

17. Corey, A.T.: "The Interrelation Between Gas and Oil Relative Permeabilities," *Producers Monthly* (November 1954) , 38.

18. Christie, M.A. and Blunt, M.: "Tenth SPE Comparative Solution Project: A Comparision of Upscaling Techniques," *SPEREE* (August 2001) **4**, 308.

19. Hewett, T.A., Suzuki, K. and Christie, M.A.: "Analytical Calculation of Coarse-Grid Corrections for Use in Pseudofunctions," *SPEJ* (1998) **3**, 293.

20. Schlumberger: *PSEUDO Reference Manual 2003A* (2003).

21. O'Sullivan, A.E.: *Modelling Simulation Error for Improved Reservoir Prediction*, Ph.D. thesis, Institute of Petroleum Engineering, Heriot-Watt University (2004).

22. Honapour, M., Koederitz, L. and Harvey, A.H.: *Relative Permeability of Petroleum Reservoirs*, CRC Press, Inc., Boca Raton (1986).

23. Willhite, G.P.: *Waterflooding*, Society of Petroleum Engineers, Richardson (1986).

24. Buckley, S.E. and Leverett, M.C.: "Mechanism of Fluid Displacement in Sands," *Trans. AIME* (March 1942) **146**, 107.

25. Barker, J.W. and Dupouy, P.: "An Analysis of Dynamic Pseudo-relative Permeability Methods for Oil-Water Flows," *Petroleum Geoscience* (1999) **5**, 385.

26. Barker, J.W. and Thibeau, S.: "A Critical Review of the Use of Pseudorelative Permeabilities for Upscaling," *SPERE* (May 1997) **12**, 138.

27. Schumaker, L.L.: *Spline Functions: Basic Theory*, J. Wiley & Sons, Inc., New York (1981).

28. Chierici, G.L.: "Novel Relations for Drainage and Imbibition Relative Permeability," *SPEJ* (June 1984) , 275.

29. Firoozabadi, A. and Aziz, K.: "Relative Permeability From Centrifuge Data," paper SPE 15059 presented at the 1986 SPE California Regional Meeting, Oakland, April 2-4.

30. Kyte, J.R. and Berry, D.W.: "New Pseudo Functions to Control Numerical Dispersion," *SPEJ* (August 1975) **5**, 269.

31. Pickup, G.E. *et al.*: "Multi-stage Upscaling: Selection of Suitable Methods," *Transport in Porous Media* (2005) **58**, 191.

32. Williams, G.J.J., Mansfield, M., MacDonald, D.G. and Bush, M.D.: "Top-Down Reservoir Modelling," paper SPE 89974 presented at the 2004 SPE Annual Technical Conference and Exhibition, Houston, September 26-29.

33. Lee, S.H., Malallah, A., Datta-Gupta, A. and Higdon, D.: "Multiscale Data Integration Using Markov Random Fields," *SPEREE* (February 2002) , 68.

34. Tran, T.T., Wen, X.H. and Behrens, R.A.: "Efficient Conditioning of 3D Fine-Scale Reservoir Model to Multiphase Production Data Using Streamline-Based Coarse-Scale Inversion and Geostatistical Downscaling," *SPEJ* (December 2001) **6**, 364.

35. Yoon, S. *et al.*: "A Multiscale Approach to Production-Data Integration Using Streamline Models," *SPEJ* (June 2001) , 182.

36. Press, W.H., Teukolsky, S.A., Vetterling, W.T. and Flannery, B.P.: *Numerical Recipes in C*, Cambridge University Press, Cambridge, second edition (1992).

37. Ding, Y.: "Scaling-up in the Vicinity of Wells in Heterogeneous Field," paper SPE 29137 presented at the 1995 SPE Symposium on Reservoir Simulation, San Antonio, February 12-15.

38. Durlofsky, L.J., Milliken, W.J. and Bernath, A.: "Scaleup in the Near-Well Region," *SPEJ* (March 2000) **5**, 110.

Appendix A- NA-Bayes Algorithm

Sambridge [6] applied the Neighbourhood Approximation to the sampling from the posterior probability distribution (PPD) in a Bayesian framework, (NA-Bayes Algorithm). Sambridge used the rejection method [36] in Gibbs sampler of MCMC [14] to draw random deviates from the 1-D conditional probability density function of the posterior probability density function, prob($\mathbf{m}|\mathbf{o}$). The only information we have from the history-matching phase is prob($\mathbf{o}|\mathbf{m}$) prob($\mathbf{m}$), which does not include the normalisation constant. However, we do not need to evaluate the normalisation constant, because the Gibbs sampler with the rejection method requires only the ratio of the 1-D conditional PPDs.

Appendix B- Details of Coarse-scale Model

In this paper, we are using history matching to estimate the relative permeabilities in the inter-well region of the model, i.e. we are estimating the relative permeabilities for cells 2 and 3 (Figure 3). We have treated the near-well regions as a special case, and have upscaled permeability and relative permeability. In a real reservoir, there is more data available in the near-well regions, so this is a reasonable procedure. Additionally, the near-well region has to be treated with care, because we have radial flow. We adopted the method described in [37] and [38] to calculate the coarse-scale well connection factor in cells 1 (injector) and 5 (producer), and the transmissibilities between cells 1 and 2, and 4 and 5. Then we extended this method to two-phase flow, to calculate the pseudo relative permeabilities for the well connections and the interfaces between the wells and adjacent cells. At the two inter-well cells (2 and 3), we calculated the absolute transmissibilities using the averaging method adopted in the PVW method of the Eclipse Pseudo Package [20].

Table 1: Min. and Max. Values for B-spline Coefficients

Basis No., j	c_j^o min.	c_j^o max.	c_j^w min.	c_j^w max.
1	1.0	1.0	0.0	0.0
2	0.3	1.0	0.0	0.4
3	0.0	1.0	0.0	0.7
4	0.0	1.0	0.0	1.0
5	0.0	0.7	0.0	1.0
6	0.0	0.0	1.0	1.0

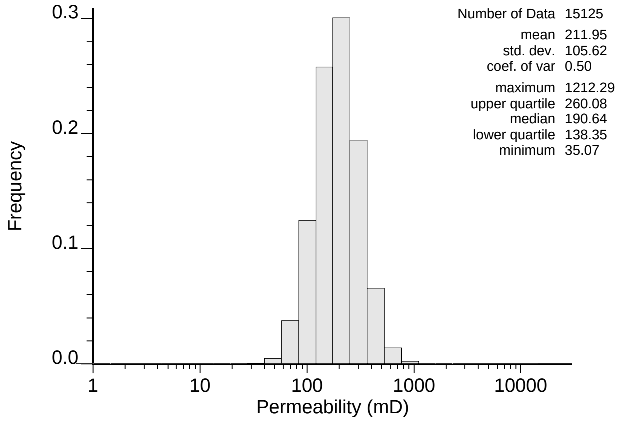

Figure 2: Permeability Histogram: Note that the x-axis is logarithmic.

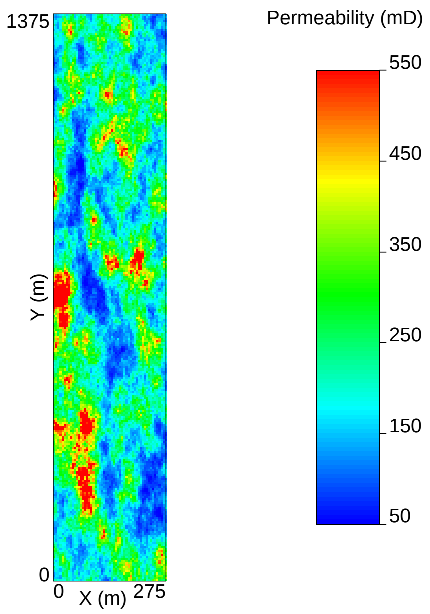

Figure 1: Permeability Distribution

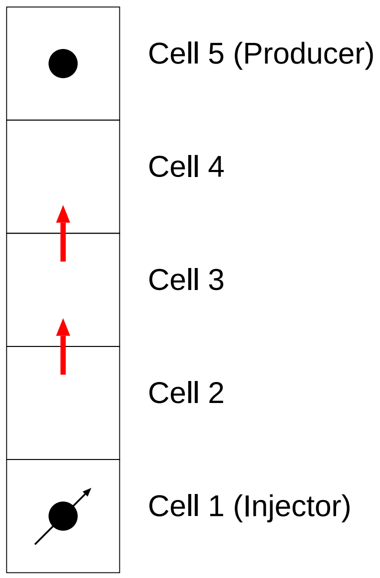

Figure 3: Coarse-Scale Model for History-Matching: Two arrows in the inter-well cells represent flow for which the relative permeabilities are adjusted during history-matching.

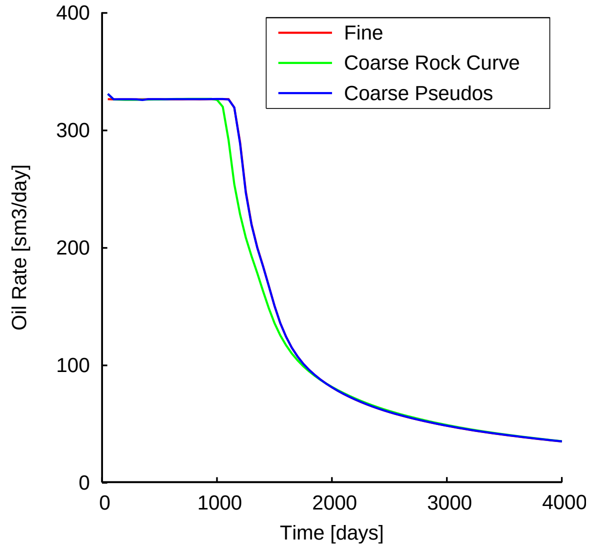

Figure 4: Oil Rate: Note that the curves of the fine-scale model and the coarse-scale model with pseudofunctions are superimposed.

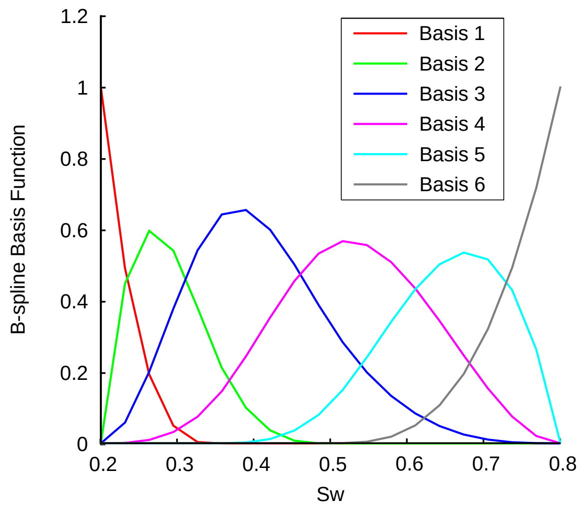

Figure 6: Normalised Cubic B-spline Basis Functions: Dimension 6, Non-uniformly Spaced Knots 0.20, 0.35, 0.50, 0.80

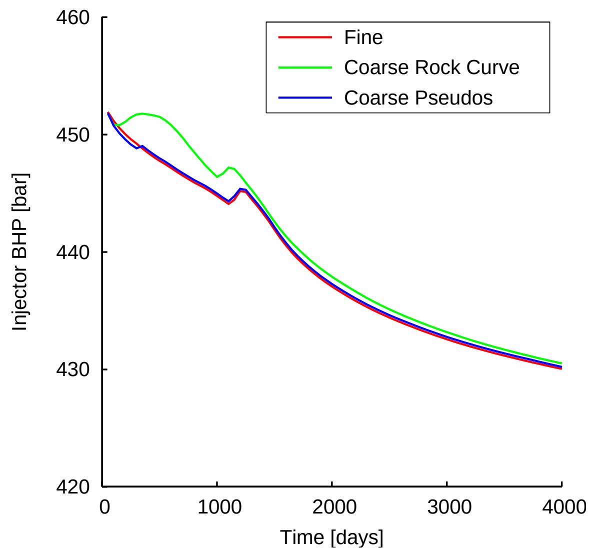

Figure 5: Injector Bottom Hole Pressure

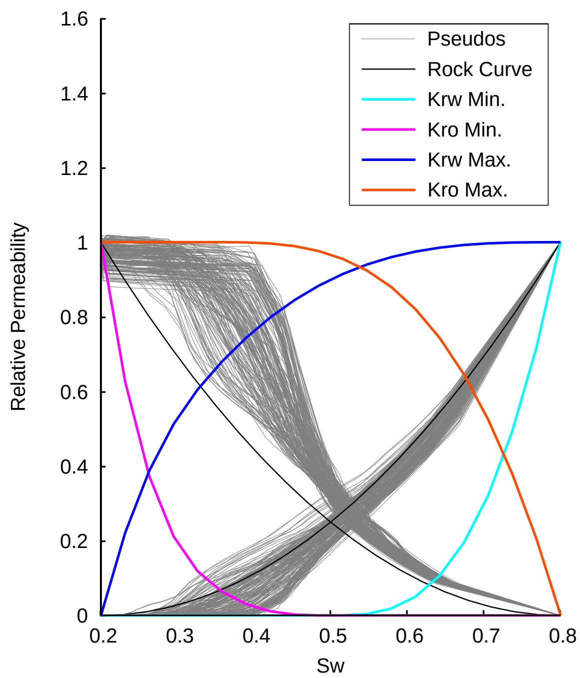

Figure 7: Range of Krw and Kro

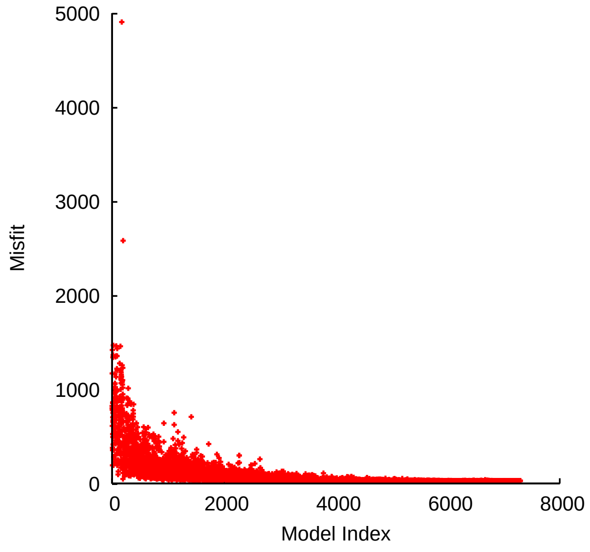

Figure 8: Misfit Values during History-Matching

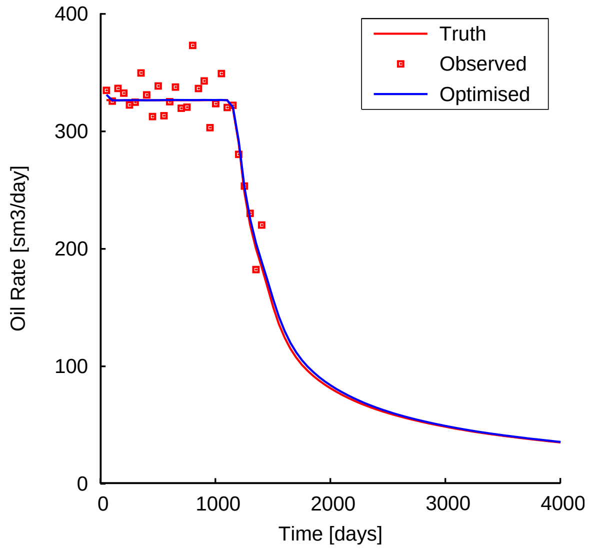

Figure 10: Oil Rate calculated using Optimised Relative Permeabilities

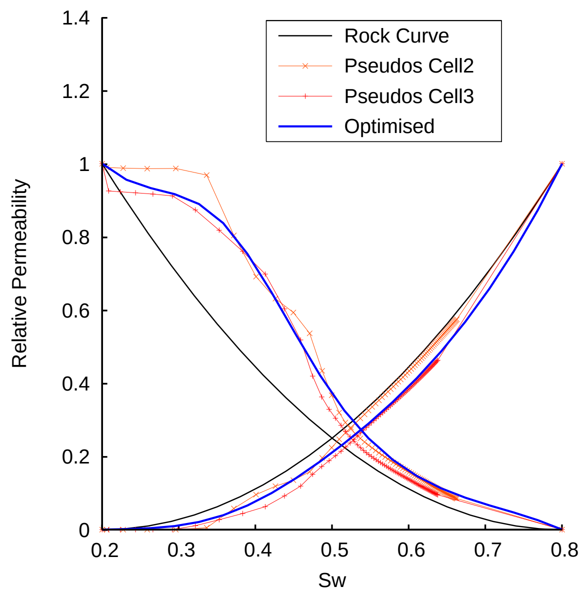

Figure 9: Optimised Relative Permeabilities

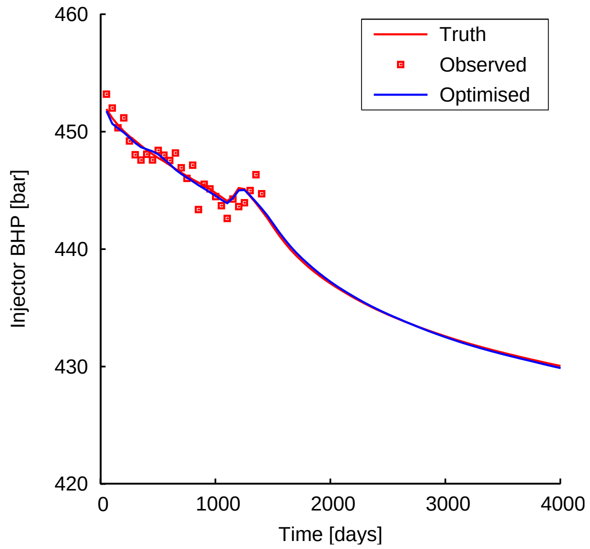

Figure 11: Injector Bottom Hole Pressure calculated using Optimised Relative Permeabilities

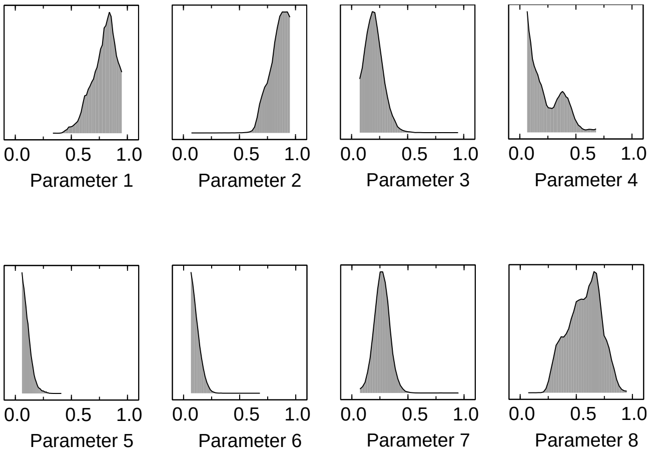

Figure 12: 1D Marginal Distribution of 100000 samples in Markov Chain: Note that each curve is scaled to the same maximum height not the same area.

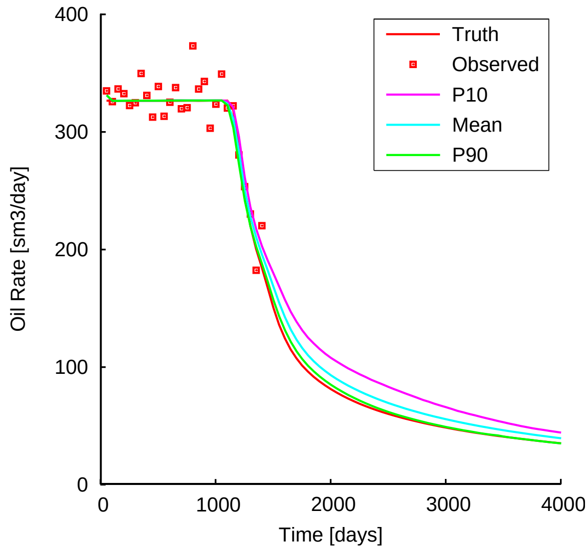

Figure 14: Uncertainty in Oil Rate

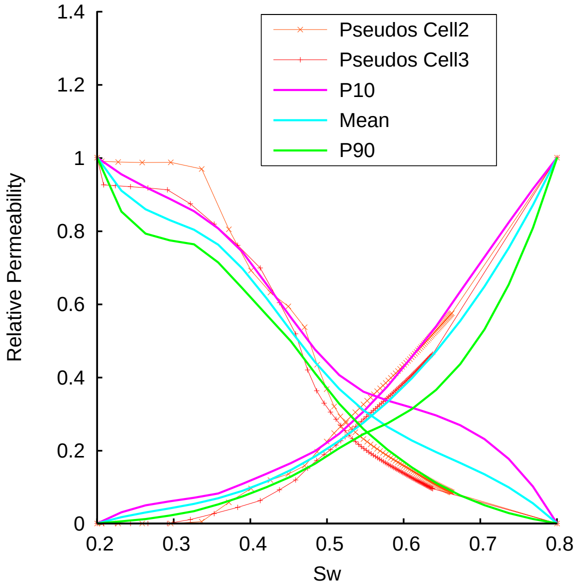

Figure 13: Uncertainty in Relative Permeabilities

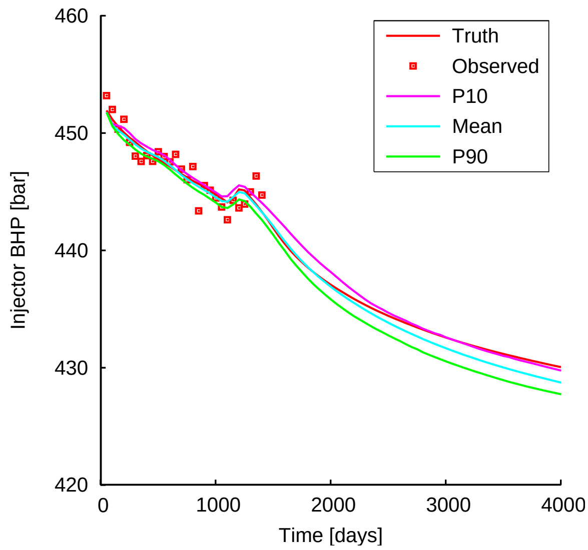

Figure 15: Uncertainty in Injector Bottom Hole Pressure